Photoelectric Measurements of Extragalactic Nebulae

Houten, C.J. van; Oort, J.H.; Hiltner, W.A.

PHOTOELECTRIC MEASUREMENTS OF EXTRAGALACTIC NEBULAE*

C. J. VAN HOUTEN, J. H. OORT, AND W. A. HILTNER
Yerkes, McDonald, and Leiden Observatories
Received June 8, 1954

ABSTRACT

This article gives the intensity distribution in nine extragalactic nebulae, measured photoelectrically with the 82-inch reflector of the McDonald Observatory. The observations were made with three different color filters and with diaphragms of various sizes.

Studies of the distribution of brightness in extragalactic nebulae have been made by Hubble (1930), Redman and Shirley (1938), Evans (1951, 1952), and De Vaucouleurs (1948), while measurements of individual objects have been made by Carpenter, Reynolds, Seyfert, Lindblad, Holmberg, Oort, and others. They were all done photographically; and, as the difference in brightness between the nucleus and the outer parts of an extragalactic nebula is considerable, a very precise determination of the gradation curves of the photographic plates was necessary. To avoid this difficulty, it was planned to measure photoelectrically the intensity distribution in a number of extragalactic nebulae. The measurements were made in January, 1948, with the 82-inch reflector of the McDonald Observatory by Hiltner, Oort, and Heyduck and are discussed in this paper. We are indebted to Dr. Strömgren for assistance with part of the measurements.

TABLE 1

A COMPARISON OF THE VARIOUS SENSITIVITY RATIOS

log	From Tracings	Mean Error	From Star	Laboratory 1948	Laboratory 1951	Hiltner Mean
L1/L2.....	0.658	±0.012	0.662	0.669	0.640	0.657
L2/L3.....	.759	± .029	.753	.751	.740	.749
L3/L4.....	0.754	±0.027	0.779	0.715	0.712	0.735

The observations were made with a refrigerated RCA 1P21 photomultiplier; the output of the cell was fed into a d.c. amplifier, and the amplified current was recorded by a Brown recorder. A diaphragm could be moved by a synchronous motor in the Cassegrain focal plane of the reflector in any arbitrary direction; three velocities were possible, 11".3, 28".1, and 70".4 per minute. Tracings were made along the major or minor axes of the nebulae, and in some cases also outside the nucleus. Most tracings were made with a color filter behind the diaphragm; the filters used were Schott Ug-2, and Corning 5850 and 3385, with effective wave lengths about 3650, 3900, and 5300 A. They will be denoted as F1, F2, and F3.

The sensitivity of the amplifier could be varied by the use of different grid leaks; the leaks used were 0.8, 4, 20, and 100 megohms, respectively. They will be denoted as L1, L2, L3, and L4. In order to insure reasonable accuracy for nucleus as well as outer parts of the nebulae, the grid leaks were changed repeatedly during a tracing. It was thought that a determination of the relative sensitivities of the grid leaks after the conclusion of the observations would be sufficient, but during the reductions it appeared that these ratios were not constant. The explanation must probably be found in changing temperature and humidity during the observations. The sensitivity ratios of the grid leaks were determined by Hiltner at the telescope from measures of stars and also in the laboratory (in 1948 and 1951). In addition, it appeared possible to determine these ratios from some tracings, where the light-variation was very regular, by extrapolating the measures on

* *Contributions from the McDonald Observatory, University of Texas*, No. 247.

both sides of the switch-over point. A comparison between the various results is shown in Table 1.

When the sensitivity ratio was determined from the tracing itself, this value was used in the reduction of the tracing. This was possible only with tracings of the nebulae NGC 221, 3115, and 4594. In all other cases the mean values were used, as found from the tracings. The values determined from stellar observations and in the laboratory were not used. This introduces some uncertainties, as these values are systematically lower. However, the differences are smaller than the deviations of the ratios from their mean value.

The sensitivity could be changed by a variation of grid leaks and also by the feedback loop. Various diaphragms were used: four were circular, with diameters of about 20″, 9″, 3″.6, and 1″.7, while rectangular diaphragms could be formed from a number of strips, five in the long and four in the short directions. No absolute determination of the areas was made, but they were measured on a moonlit sky, so that the relative transmission could be ascertained. These values are collected in Table 2 in the columns marked "Size"; the length indicated as 100″ and the width indicated as 8″ were arbitrarily assumed to be accurately 100″ and 8″. The dark deflection was determined before and after each tracing; measures of the night sky were made only once a night for each nebula. However, the sky appeared not to be constant during this time. This caused serious errors in the reduction of the faintest parts of the nebulae; sometimes the resulting intensities of the outermost parts were negative. In these cases the sky intensity was altered until the marginal values corresponded to those of other tracings. The effects of wrong sky cor-

TABLE 2

AREAS OF DIAPHRAGMS

Length		Width		Area of Circular Diaphragm	
Called	Size	Called	Size	Called	Size
100″.....	100″	8″.....	8″	8″	300(″)²
50.....	51.2	4.....	3.31	4.....	64.2
25.....	27.5	2.....	1.54	2.....	10.2
12.....	13.1	1.....	1.06	1.....	2.2
6.....	6.38				

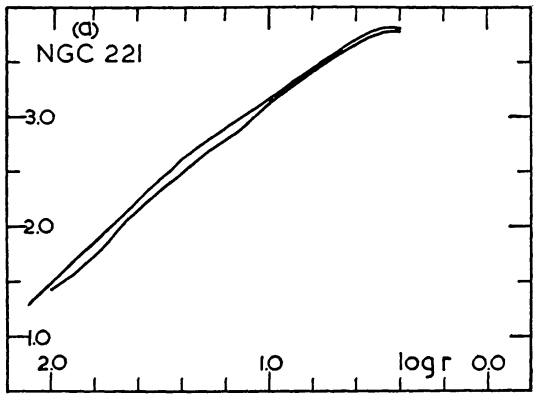

FIG. 1.—Position angles (p.a.) are counted from north through east, as usual. In each graph the abscissa, x or y, increases in the direction p.a. +180°. The letter x is used for the co-ordinates parallel to the major axis, while y indicates the co-ordinates parallel to the minor axis. Both are expressed in seconds of arc. Ordinates are logarithms of intensities. In several cases where the nebulae appeared to be symmetrical, the two halves of the intensity-curves were averaged. Log I was then plotted against log x or log y. When a rectangular diaphragm was used, it was always placed in such a way that the short axis was in the direction in which the tracing was done. *a*, NGC 221, major and minor axes, no filter. P.a. 90° and 0°, respectively; D4″.

rections are clearly seen in some of the tracings of Figures 1–5. The sky has only a very small influence on the brightness of the inner parts of the nebulae; accordingly, these values are much more reliable than the parts of low intensity.

The unit of intensity used in this article is a hundredth part of the vertical scale of the recorder paper when the instrument was used with the largest grid leak and the greatest

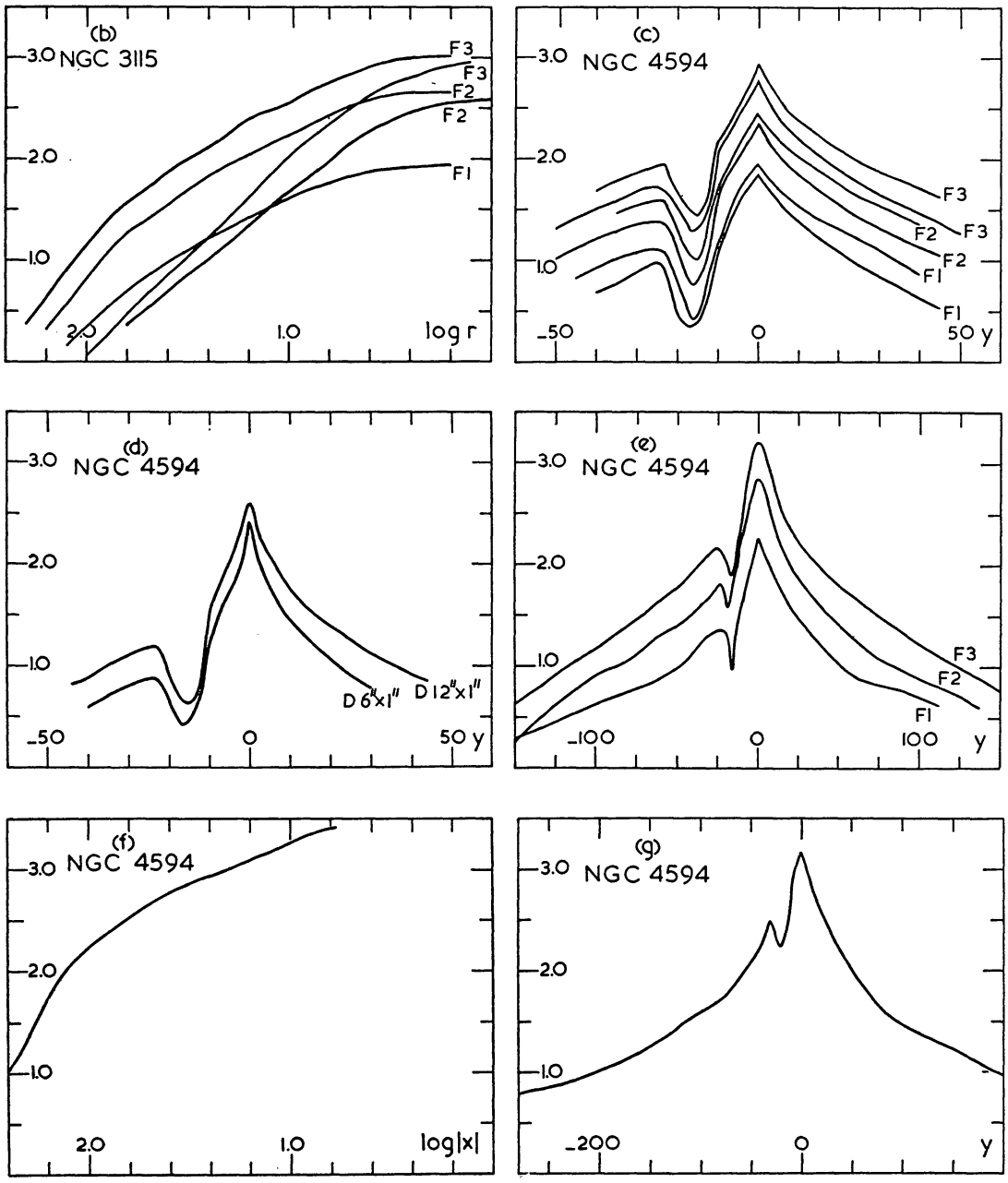

FIG. 2.—*b*, NGC 3115, major and minor axes. P.a. 44°.1 with D4″ and 314°.1 with D12″ × 4″, respectively. *c*, NGC 4594, minor axis. P.a. 0°; D50″ × 1″ and D100″ × 1″. *d*, NGC 4594, minor axis. P.a. 0°; F3. End of measures in twilight. *e*, NGC 4594, minor axis. P.a. 0°; D50″ × 4″. Sky corrections uncertain. *f*, NGC 4594, major axis. P.a. 90°; F3. D8″. *g*, NGC 4594, minor axis. P.a. 0°; F3. D100″ × 4″. Measures of dark current incomplete. Otherwise the arrangement is the same as in Fig. 1.

sensitivity. This unit is, of course, intrinsically variable, but no better method was possible, because the sensitivity variations were not known. On some nights comparison stars near the nebulae were measured and compared with stars in the polar cap. Since, however, no extinction measures were made, an accurate determination of the zero point of brightness was not possible. All measures were corrected for extinction by means

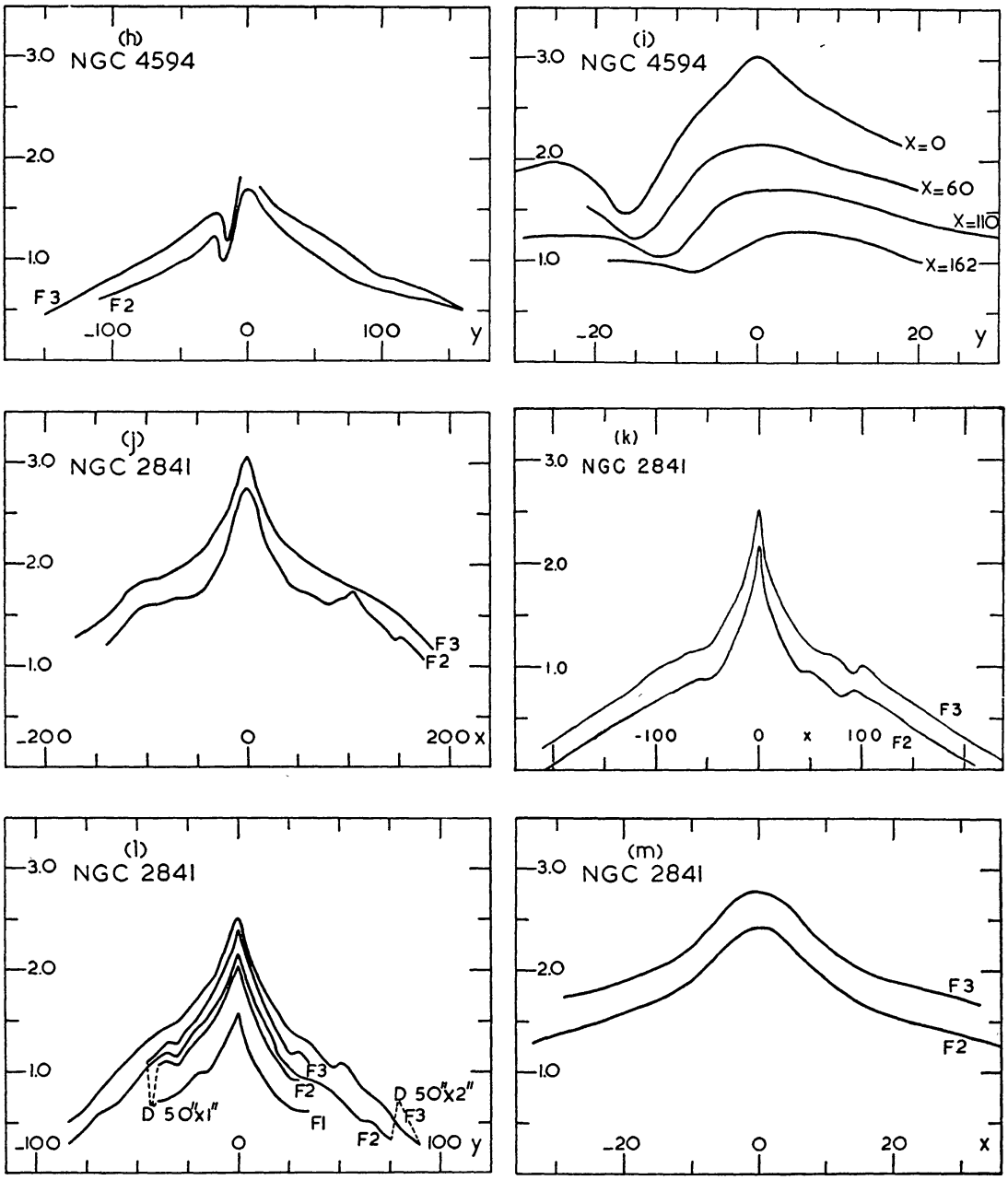

FIG. 3.—*h*, NGC 4594. Tracings across shadow band 1′ outside nucleus. P.a. 0°; D50″ × 2″. *i*, NGC 4594. Tracings across shadow band. P.a. 0°; F3; D25″ × 4″. Measures of dark current incomplete. *j*, NGC 2841, major axis. P.a. 330°; D8″. *k*, NGC 2841, major axis. P.a. 330°; D12″ × 4″. *l*, NGC 2841, minor axis. P.a. 60°; D50″ × 2″ and D50″ × 1″. *m*, NGC 2841, major axis. P.a. 330°; D4″. Otherwise the arrangement is the same as in Fig. 1.

of the well-known formula

$$m = m_0 + K \sec z .$$

The values used for K were 0.55, 0.24, and 0.15 mag. for filters F1, F2, and F3, respectively. All magnitudes were reduced to the zenith, i.e., they were diminished by K (sec

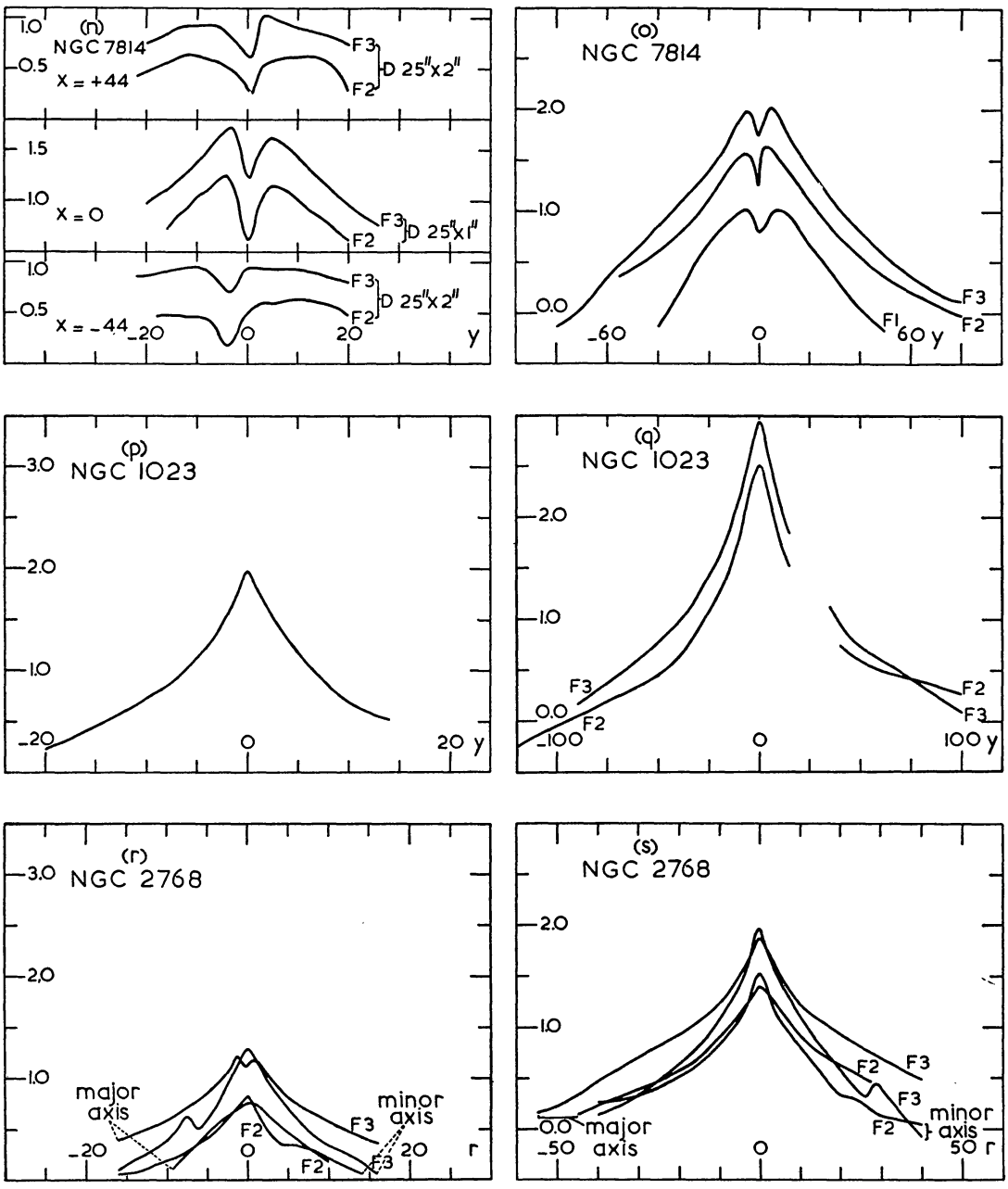

FIG. 4.—*n*, NGC 7814. Tracings across shadow band. P.a. 45″. For $x = 0$, D25″ × 1″; for $x = \pm 44$″, D25″ × 2″. *o*, NGC 7814, minor axis. P.a. 45°; D25″ × 4″. *p*, NGC 1023, minor axis. P.a. 353°.5; F3; D1″. *q*, NGC 1023, minor axis. P.a. 353°.5; D4″. Corrections for sky and dark current uncertain. Star in slit at about $y = 25$″. *r*, NGC 2768, major and minor axes. P.a. 10° and 100°, respectively; D1″. *s*, NGC 2768, major and minor axes. P.a. 10° and 100°, respectively; D2″. Otherwise the arrangement is the same as in Fig. 1.

$z - 1$). The brightness found in this way is not independent of the value of the absorption coefficient, but only a mean extinction coefficient was used; in this way the corrections, and also the errors in the corrections, are smaller.

The results of the color measures of the standard stars and the nuclei of the nebulae are shown in Table 3. It follows from Table 3 that the colors of the nuclei of the nebulae

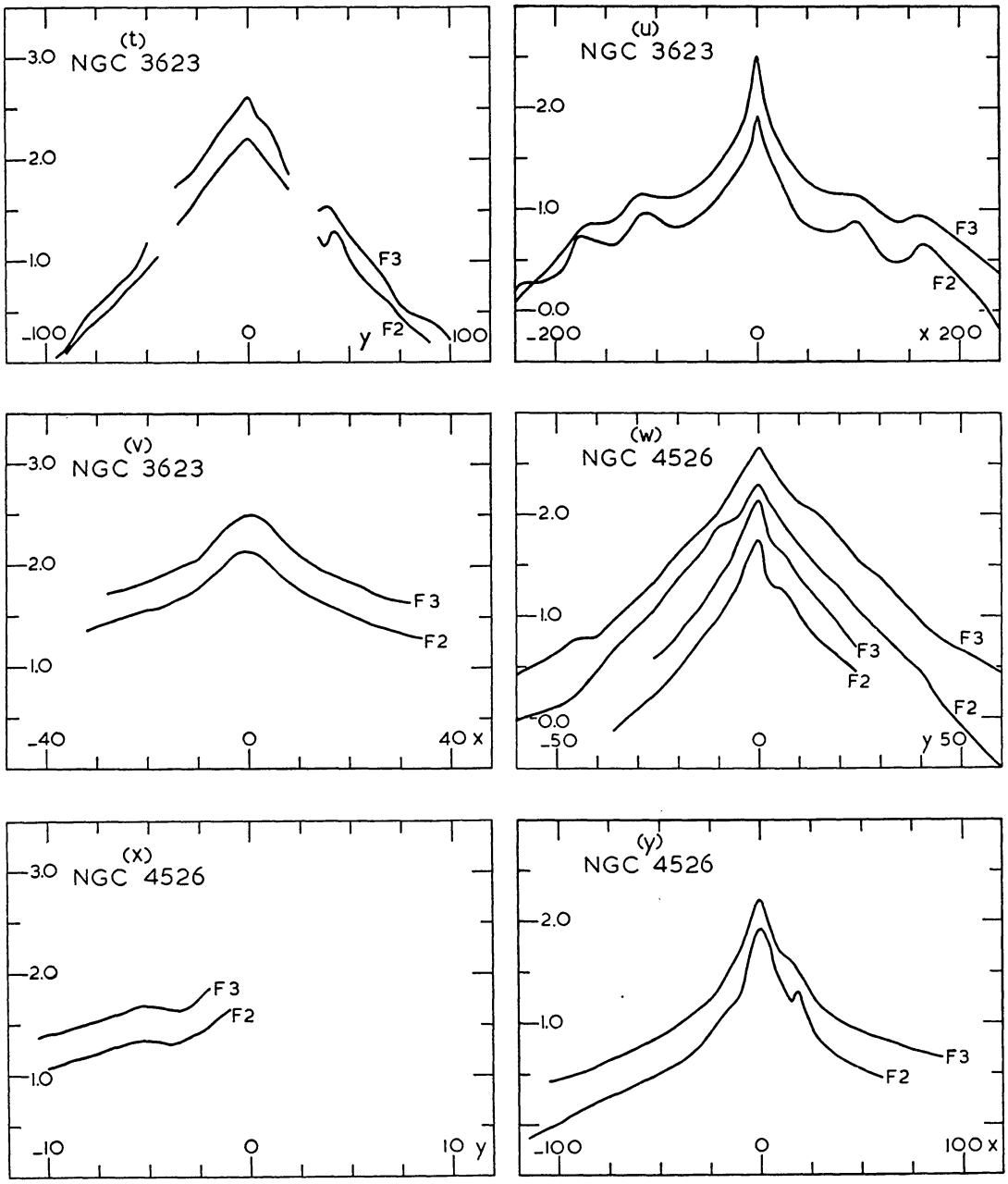

FIG. 5.—*t*, NGC 3623, minor axis. P.a. 82°; D50″ × 4″. Star in slit at approximately $y = -40''$ and $y = +25''$. *u*, NGC 3623, major axis. P.a. 352°; D12″ × 4″. *v*, NGC 3623, major axis. P.a. 352°; D4″. *w*, NGC 4526, minor axis. P.a. 20°.5; D25″ × 4″ and D12″ × 1″. *x*, NGC 4526, minor axis. Tracings across shadow band. P.a. 20°.5; D12″ × 1″. *y*, NGC 4526, major axis. P.a. 290°.5; D6″ × 4″. Otherwise the arrangement is the same as in Fig. 1.

NGC 2841

NGC 3623

NGC 4526

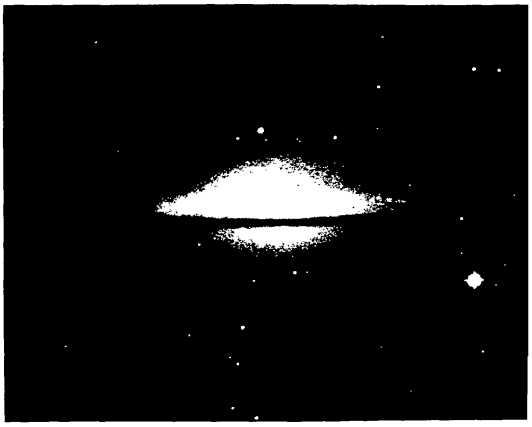

NGC 4594

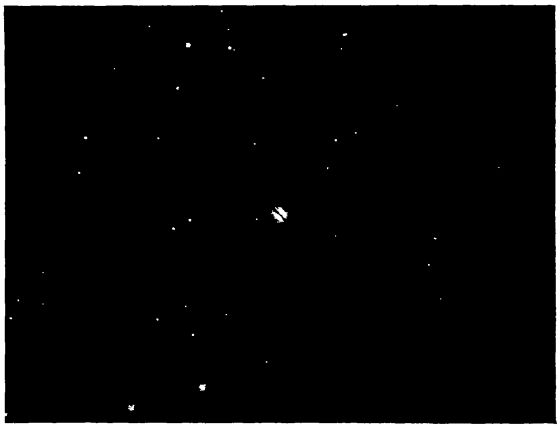

NGC 7814

FIG. 6.—Extragalactic nebulae

correspond to a spectral type of about G6 or G7. The brightness of the standard stars as measured with F2 was compared with the HD photographic magnitudes. The result is shown in Table 4. The last two columns of Table 4 show systematic differences, depending on the spectral type. This makes possible the reduction of the F2 intensities to the photographic system. The result is that a star of spectral type G6 and photographic magnitude 10.0 would have a brightness of log $I = 4.00$ with F3 in our system.

The nebulae studied in this investigation are NGC 221, 3115, 4594, 2841, 1023, 2768, 3623, 4526, and 7814. Types, magnitudes, and dimensions are given in Table 5. These

TABLE 3

COLORS OF STANDARD STARS AND NUCLEI OF NEBULAE

Standard Star	Sp.	log F3/F2	log F1/F2	NGC	log F3/F2	log F1/F2
BD+80°80.....	K5	+0.87	−0.83	221.....	+0.36	−0.53
BD+80°121.....	K0	+ .55	− .60	3115.....	+ .40	− .52
BD+80°159.....	F0	+ .02	− .37	4594.....	+ .43	−0.53
BD+80°233.....	F8	+ .11	− .41	2841.....	+ .39	.....
BD+80°338.....	K0	+0.60	−0.68	1023.....	+ .47	.....
				2768.....	+ .45	.....
				3623.....	+0.41	.....

TABLE 4

GENERAL INFORMATION ABOUT THE STANDARD STARS

Standard Star	Sp.	log I (F3)	Δm, HD	Δm, F2
BD+80°80.....	K5	4.51	0.00	0.00
BD+80°121.....	K0	4.63	−1.09	−1.12
BD+80°159.....	F0	4.28	−1.04	−1.56
BD+80°233.....	F8	4.24	−0.82	−1.24
BD+80°338.....	K0	4.64	−0.93	−1.03

TABLE 5

GENERAL INFORMATION ABOUT THE NEBULAE

Nebula	Type	m_{pg}	Diameters
NGC 221.....	E	9.5	2′.6 × 2′.1
NGC 1023.....	SBa	11.2	6.9 × 1.3
NGC 2768.....	E5	12.0	1.5 × 0.7
NGC 2841.....	Sb	10.5	6.0 × 1.6
NGC 3115.....	E7	9.8	4.0 × 1.0
NGC 3623.....	Sb	10.5	8.0 × 2.0
NGC 4526.....	Sa	10.7	6.0 × 1.2
NGC 4594.....	Sa	8.1	7.0 × 1.5
NGC 7814.....	Sa	12.4	3.0 × 0.8

were taken from Shapley and Miss Ames's catalogue (1932). Reproductions of NGC 2841, 3623, 4526, 4594, and 7814 are shown in Figure 6. The other nebulae have an entirely smooth structure.

The results of the tracings are collected in Table 6 and in Figures 1–5. As a rule the logarithm of the brightness (I) was tabulated as a function of the distance to the nucleus. Co-ordinates parallel to the major axis are denoted by x, those parallel to the minor axis by y. Both are expressed in seconds of arc and are counted from the nucleus as zero point. Only when the intensity distribution in the tracing was very regular, was log I compared with log x or log y. This has been done with NGC 221, NGC 3115, and the major axis of NGC 4594. Here, symmetry relative to the nucleus was assumed, and, accordingly, the two sides were combined in one figure (Figs. 1, *b*, and 2, *f*). The values in Table 6 were obtained by drawing a smooth line through the tracing on the recorder

TABLE 6

Photometry of Extragalactic Nebulae

(a)	NGC 221*, No Filter			
	Minor Axis		Major Axis	
log r	D 2"	D 4"	D 2"	D 4"
- ∞	3.50		3.40	3.83
0.4	2.89	3.81	3.14	3.79
0.5	2.77	3.79	3.05	3.75
0.6	2.64	3.70	2.89	3.66
0.7	2.50	3.57	2.74	3.54
0.8	2.35	3.43	2.58	3.41
0.9	2.20	3.29	2.42	3.26
1.0	2.06	3.16	2.30	3.11
1.1	1.88	3.03	2.15	2.93
1.2	1.71	2.89	1.99	2.78
1.3	1.51	2.75	1.85	2.64
1.4	1.33	2.59	1.71	2.48
1.5		2.42	1.54	2.32
1.6		2.23	1.34	2.15
1.7		2.04	1.11	1.94
1.8		1.85	0.86	1.73
1.9		1.68		1.55
2.0		1.48		1.42
2.1		1.29		

*Since the sensitivity of the amplifier was not recorded the zero point is not known.

(b)	NGC 3115				
	Minor Axis D 12"x4"		Major Axis ; D 4"		
log r	F2	F3	F1	F2	F3
- ∞	2.62	3.02	1.98	2.71	3.05
0.2	2.55	2.92	1.94	2.67	3.02
0.4	2.45	2.80	1.92	2.65	2.99
0.5	2.37	2.73	1.90	2.63	2.96
0.6	2.27	2.62	1.87	2.59	2.91
0.7	2.13	2.48	1.83	2.52	2.84
0.8	1.97	2.34	1.76	2.43	2.75
0.9	1.82	2.19	1.69	2.33	2.66
1.0	1.68	2.02	1.62	2.23	2.55
1.1	1.53	1.83	1.53	2.14	2.47
1.2	1.35	1.63	1.43	2.04	2.39
1.3	1.17	1.42	1.32	1.94	2.25
1.4	1.01	1.22	1.22	1.82	2.11
1.5	0.86	1.04	1.10	1.69	1.99
1.6	0.69	0.87	0.97	1.54	1.86
1.7	0.53	0.68	0.84	1.40	1.71
1.8	0.36	0.48	0.70	1.28	1.57
1.9		0.26	0.54	1.08	1.39
2.0		0.05	0.35	0.82	1.15
2.1			0.16	0.56	0.91
2.2				0.32	0.64
2.3					0.37

(c) and (d)	NGC 4594, Minor Axis							
	D 100"x1"			D 50"x1"			D 12"x1"	D 6"x1"
y	F1	F2	F3	F1	F2	F3	F3	F3
-50					1.01	1.31		
-45	0.82				1.11	1.41		
-40	0.92		1.68	0.68	1.21	1.50	0.89	0.58
-35	1.02	1.46	1.78	0.76	1.27	1.57	1.01	0.71
-30	1.06	1.53	1.85	0.88	1.35	1.68	1.10	0.80
-25	1.10	1.58	1.92	0.98	1.37	1.72	1.17	0.87
-23	1.08	1.58	1.94	0.90	1.36	1.70	1.19	0.87
-20	0.78	1.30	1.67	0.47	1.09	1.52	0.90	0.66
-17	0.45	1.06	1.51	0.35	0.78	1.29	0.67	0.42
-16	0.42	1.03	1.47	0.37	0.76	1.29	0.65	0.45
-15	0.46	1.01	1.44	0.39	0.80	1.31	0.63	0.46
-13	0.77	1.23	1.57	0.55	1.00	1.44	0.72	0.63
-10	1.17	1.75	2.16	1.13	1.65	2.08	1.52	1.23
- 5	1.69	2.14	2.52	1.58	2.06	2.42	2.03	1.73
0	1.95	2.45	2.93	1.85	2.35	2.79	2.60	2.42
5	1.70	2.20	2.60	1.59	2.04	2.42	2.07	1.77
10	1.54	2.02	2.39	1.39	1.86	2.20	1.76	1.45
15	1.41	1.89	2.24	1.23	1.70	2.04	1.54	1.25
20	1.31	1.76	2.10	1.09	1.56	1.90	1.39	1.07
25	1.21	1.63	1.99	0.95	1.42	1.77	1.25	0.90
30	1.11	1.55	1.88	0.84	1.32	1.65	1.12	0.77
35	0.97	1.45	1.80	0.74	1.23	1.56	1.02	
40	0.87	1.36	1.72	0.63	1.13	1.47	0.92	
45			1.63	0.54	1.05	1.38		
50						1.27		

TABLE 6 (Cont'd)

(e) NGC 4594, Minor Axis							
D 50'x4'							
y	F1	F2	F3	y	F1	F2	F3
-170	0.19			10	1.89	2.38	2.73
-160	0.23	0.09		20	1.61	2.02	2.39
-150	0.28	0.25		30	1.36	1.76	2.12
-140	0.35	0.40	0.73	40	1.20	1.58	1.96
-130	0.42	0.54	0.85	50	1.05	1.43	1.80
-120	0.49	0.68	0.97	60	0.92	1.31	1.68
-110	0.56	0.80	1.06	70	0.84	1.14	1.55
-100	0.62	0.91	1.17	80	0.80	1.05	1.45
- 90	0.69	0.97	1.28	90	0.75	0.98	1.33
- 80	0.75	1.05	1.39	100	0.70	0.89	1.23
- 70	0.80	1.19	1.52	110	0.64	0.83	1.14
- 60	0.89	1.30	1.65	120	0.59	0.75	1.04
- 50	0.99	1.39	1.76	130		0.67	0.95
- 40	1.15	1.52	1.93	140		0.59	0.85
- 30	1.31	1.68	2.10	150		0.52	0.76
- 20	1.33	1.66	2.05	160		0.47	0.66
- 15	1.16	1.87	1.93	170		0.41	0.56
- 10	1.62	2.29	2.37	180			0.46
0	2.24	2.85	3.21				

(f) NGC 4594 Major Axis	
D 8'	
Log |x|	F3
- ∞	3.47
0.8	3.41
0.9	3.35
1.0	3.28
1.1	3.19
1.2	3.11
1.3	3.03
1.4	2.93
1.5	2.86
1.6	2.77
1.7	2.67
1.8	2.53
1.9	2.38
2.0	2.23
2.1	2.04
2.2	1.75
2.3	1.34
2.4	1.02
2.5	0.69

(g) NGC 4594, Minor Axis			
D 100'x4'			
y	F3	y	F3
-290	0.76	-40	2.23
-280	0.79	-30	2.49
-270	0.81	-20	2.24
-260	0.83	-10	2.79
-250	0.85	0	3.17
-240	0.87	10	2.87
-230	0.91	20	2.59
-220	0.94	30	2.37
-210	0.98	40	2.20
-200	1.01	50	2.02
-190	1.05	60	1.85
-180	1.09	70	1.72
-170	1.14	80	1.63
-160	1.19	90	1.55
-150	1.25	100	1.47
-140	1.31	110	1.41
-130	1.39	120	1.36
-120	1.46	130	1.31
-110	1.52	140	1.27
-100	1.59	150	1.23
- 90	1.65	160	1.18
- 80	1.72	170	1.12
- 70	1.81	180	1.06
- 60	1.95	190	1.01
- 50	2.09	200	0.98

(h) NGC 4594, Tracings Across Shadow Band					
D 50'x2'. |x|=60					
y	F2	F3	y	F2	F3
-150		0.45	- 5	1.62	1.81
-140		0.51	0	1.69	
-130		0.59	10	1.54	1.72
-120		0.66	20	1.38	1.55
-110	0.60	0.74	30	1.24	1.45
-100	0.64	0.81	40	1.14	1.36
- 90	0.70	0.88	50	1.05	1.29
- 80	0.76	0.96	60	0.96	1.21
- 70	0.82	1.03	70	0.87	1.13
- 60	0.90	1.11	80	0.80	1.04
- 50	0.97	1.20	90	0.74	0.91
- 40	1.04	1.31	100	0.70	0.83
- 30	1.16	1.41	110	0.67	0.81
- 25	1.23	1.45	120	0.63	0.76
- 20	1.02	1.45	130	0.61	0.72
- 18	0.99	1.37	140	0.57	0.66
- 15	1.07	1.19	150	0.54	0.59
- 10	1.39	1.43	160	0.51	0.52

TABLE 6 (Cont'd)

(i) NGC 4594; Tracings Across Shadow Band									
D 25'x4' ; F3									
y	x=0	|x|=60	|x|=110	|x|=162	y	x=0	|x|=60	|x|=110	|x|=162
-32	1.84				0	3.02	2.15	1.69	1.22
-30	1.88				2	2.94	2.14	1.71	1.27
-28	1.92		1.23		4	2.78	2.11	1.72	1.30
-26	1.96		1.24		6	2.66	2.04	1.70	1.30
-24	1.95		1.24		8	2.56	2.00	1.67	1.29
-22	1.90		1.24		10	2.46	1.94	1.64	1.26
-20	1.79	1.47	1.24		12	2.36	1.90	1.60	1.23
-18	1.56	1.35	1.22	1.00	14	2.29	1.85	1.55	1.18
-16	1.48	1.24	1.17	0.99	16	2.22	1.81	1.50	1.12
-14	1.59	1.24	1.08	0.98	18	2.15	1.76	1.44	1.06
-12	1.90	1.39	1.05	0.96	20		1.71	1.39	1.01
-10	2.18	1.64	1.10	0.93	22			1.36	
- 8	2.40	1.84	1.27	0.91	24			1.33	
- 6	2.57	1.99	1.45	0.95	26			1.30	
- 4	2.75	2.08	1.60	1.03	28			1.27	
- 2	2.92	2.12	1.65	1.13	30			1.25	

(j) and (k) NGC 2841; Major Axis									
	D 8'		D 12'x4'			D 8'		D 12'x4'	
x	F2	F3	F2	F3	x	F2	F3	F2	F3
-230			-0.17		10	2.52	2.75	1.59	1.90
-220			-0.08		20	2.20	2.47	1.32	1.66
-210			-0.01	0.22	30	2.00	2.30	1.11	1.46
-200			0.06	0.29	40	1.83	2.19	0.96	1.31
-190			0.13	0.35	50	1.76	2.10	0.95	1.21
-180			0.20	0.42	60	1.72	2.03	0.89	1.14
-170		1.28	0.26	0.50	70	1.67	1.95	0.79	1.12
-160		1.33	0.32	0.55	80	1.61	1.89	0.72	1.06
-150		1.40	0.39	0.61	90	1.66	1.84	0.77	0.94
-140	1.20	1.47	0.44	0.65	100	1.70	1.80	0.75	1.02
-130	1.29	1.56	0.50	0.72	110	1.65	1.76	0.68	0.96
-120	1.42	1.71	0.56	0.82	120	1.52	1.70	0.62	0.87
-110	1.53	1.78	0.62	0.91	130	1.45	1.63	0.56	0.77
-100	1.59	1.83	0.68	0.99	140	1.33	1.57	0.50	0.70
- 90	1.60	1.85	0.73	1.01	150	1.29	1.51	0.41	0.64
- 80	1.63	1.88	0.77	1.07	160	1.22	1.41	0.34	0.59
- 70	1.67	1.94	0.84	1.12	170	1.13	1.32	0.28	0.52
- 60	1.67	2.00	0.88	1.14	180		1.21	0.22	0.45
- 50	1.70	2.09	0.88	1.20	190			0.16	0.38
- 40	1.80	2.19	0.95	1.34	200			0.10	0.31
- 30	1.97	2.36	1.12	1.52	210			0.05	0.26
- 20	2.21	2.52	1.35	1.70	220			0.00	0.19
- 10	2.55	2.79	1.63	2.02	230				0.14
0	2.75	3.05	2.17	2.52	240				0.07

TABLE 6 (Cont'd)

(l) NGC 2841; Minor Axis			
D 50"x1"			
y	F1	F2	F3
-45			1.10
-40	0.71	1.07	1.18
-35	0.72	1.10	1.29
-30	0.78	1.07	1.28
-25	0.88	1.21	1.43
-20	0.99	1.33	1.54
-15	0.99	1.42	1.70
-10	1.17	1.58	1.87
- 5	1.36	1.82	2.08
0	1.57	2.04	2.39
5	1.22	1.70	2.10
10	1.03	1.46	1.81
15	0.86	1.24	1.59
20	0.73	1.09	1.37
25	0.65	0.94	1.19
30	0.61	0.92	1.20
35	0.61		1.09

(l) NGC 2841; Minor Axis		
D 50"x2"		
y	F2	F3
-80	0.36	0.56
-70	0.57	0.78
-60	0.68	1.00
-50	0.92	1.22
-40	1.14	1.39
-30	1.16	1.49
-20	1.44	1.73
-10	1.68	2.02
0	2.16	2.51
10	1.60	1.94
20	1.16	1.57
30	0.95	1.34
40	0.89	1.18
50	0.73	1.08
60	0.52	0.86
70	0.42	0.70
80		0.44
90		0.28

(m) NGC 2841; Major Axis		
D 4"		
Log |x|	F2	F3
- ∞		2.78
0.4	2.37	2.75
0.5	2.35	2.73
0.6	2.31	2.69
0.7	2.23	2.60
0.8	2.15	2.50
0.9	2.04	2.38
1.0	1.92	2.26
1.1	1.80	2.12
1.2	1.69	2.02
1.3	1.58	1.92
1.4	1.47	1.82
1.5	1.35	1.71
1.6	1.23	

(n) NGC 7814; Minor Axis		
D 25"x1"		
y	F2	F3
-20		0.97
-18		1.04
-16	0.72	1.10
-14	0.85	1.19
-12	0.92	1.28
-10	1.04	1.38
- 8	1.09	1.50
- 6	1.19	1.60
- 4	1.24	1.70
- 3	1.15	1.72
- 2	1.02	1.63
- 1	0.77	1.48
0	0.62	1.25
0.5	0.63	1.23
1	0.69	1.29
2	0.92	1.44
3	1.03	1.53
4	1.11	1.59
5	1.15	1.62
6	1.14	1.60
8	1.10	1.53
10	1.01	1.43
12	0.92	1.33
14	0.86	1.24
16	0.78	1.14
18	0.70	1.05
20	0.62	0.96
22		0.89
24		0.82
26		0.77

(n) NGC 7814; Tracings Across Shadow Band				
D 25"x2"				
	x=+44		x=-44	
y	F2	F3	F2	F3
-22	0.43			0.86
-20	0.47	0.75		0.86
-18	0.51	0.79	0.47	0.88
-16	0.55	0.84	0.48	0.90
-14	0.60	0.89	0.48	0.92
-12	0.63	0.91	0.47	0.94
-10	0.62	0.92	0.47	0.95
- 8	0.60	0.93	0.44	0.92
- 7	0.58	0.93	0.39	0.87
- 6	0.57	0.92	0.32	0.82
- 5	0.54	0.89	0.23	0.76
- 4	0.51	0.84	0.18	0.71
- 3	0.48	0.79	0.21	0.72
- 2	0.44	0.74	0.32	0.80
- 1	0.39	0.69	0.44	0.91
0	0.31	0.63	0.50	0.93
1	0.26	0.63	0.54	0.94
2	0.43	0.85	0.57	0.94
3	0.53	1.01	0.59	0.93
4	0.55	1.02	0.59	0.93
6	0.59	0.98	0.60	0.93
8	0.61	0.95	0.62	0.93
10	0.61	0.91	0.63	0.92
12	0.62	0.88	0.62	0.91
14	0.61	0.86	0.61	0.89
16	0.56	0.83	0.59	0.85
18	0.45	0.79	0.55	0.83
20	0.29	0.73	0.48	0.80

TABLE 6 (Cont'd)

(o) NGC 7814; Minor Axis

D 25'x4'

y	F1	F2	F3
-110			-0.40
-100			-0.32
- 90			-0.23
- 80		0.08	-0.13
- 70		0.19	0.03
- 60		0.30	0.32
- 50		0.43	0.58
- 40	-0.14	0.60	0.84
- 30	0.27	0.81	1.10
- 20	0.69	1.11	1.38
- 10	0.95	1.46	1.77
- 5	1.02	1.56	1.98
0	0.80	1.25	1.74
5	1.00	1.61	2.02
10	1.00	1.45	1.84
20	0.67	1.12	1.43
30	0.36	0.80	1.09
40	0.05	0.56	0.81
50	-0.18	0.35	0.56
60		0.21	0.36
70		0.08	0.21
80		-0.02	0.12
90			0.05
100			-0.01
110			-0.07
120			-0.13
130			-0.20
140			-0.28
150			-0.35

(p) NGC 1023

D 1'; Minor Axis

y	F3
-20	0.23
-18	0.31
-16	0.40
-14	0.50
-12	0.60
-10	0.72
- 8	0.85
- 6	1.02
- 4	1.24
- 2	1.54
0	1.97
2	1.62
4	1.31
6	1.07
8	0.85
10	0.69
12	0.59
14	0.52

(q) NGC 1023

D 4'; Minor Axis

y	F2	F3
-120	-0.25	-0.16
-110	-0.16	-0.06
-100	-0.06	0.05
- 90	0.03	0.16
- 80	0.14	0.30
- 70	0.23	0.44
- 60	0.33	0.60
- 50	0.44	0.77
- 40	0.62	0.98
- 30	0.92	1.25
- 20	1.25	1.61
- 10	1.81	2.19
0	2.51	2.94
10	1.84	2.19
20	1.34	
30		
40	0.76	0.99
50	0.60	0.73
60	0.50	0.60
70	0.44	0.49
80	0.39	0.35
90	0.32	0.22
100	0.27	0.06
110	0.21	0.01

(r) NGC 2768

	D 1', Minor Axis		D 1', Major Axis	
r	F2	F3	F2	F3
-16	0.05	0.10		0.39
-14	0.07	0.19		0.45
-12	0.13	0.27		0.51
-10	0.19	0.39		0.59
- 8	0.25	0.59	0.21	0.69
- 6	0.37	0.51	0.38	0.80
- 4	0.47	0.71	0.53	0.92
- 2	0.66	1.04	0.66	1.11
0	0.82	1.29	0.76	1.13
2	0.56	1.04	0.68	1.10
4	0.35	0.81	0.54	0.89
6	0.34	0.62	0.40	0.75
8	0.30	0.45	0.30	0.67
10	0.21	0.34	0.19	0.58
12	0.13	0.27		0.51
14	0.06	0.18		0.43
16		0.06		0.37

(s) NGC 2768

	D 2', Minor Axis		D 2', Major Axis	
r	F2	F3	F2	F3
-55				0.16
-50				0.22
-45		0.04	0.14	0.32
-40	0.25	0.14	0.23	0.47
-35	0.26	0.22	0.29	0.59
-30	0.31	0.34	0.38	0.70
-25	0.40	0.49	0.47	0.81
-20	0.50	0.64	0.57	0.92
-15	0.64	0.81	0.70	1.07
-10	0.84	1.09	0.90	1.23
- 5	1.08	1.42	1.11	1.51
0	1.52	1.97	1.41	1.87
5	1.06	1.45	1.18	1.49
10	0.79	1.12	0.90	1.22
15	0.55	0.79	0.75	1.07
20	0.32	0.57	0.62	0.93
25	0.26	0.34	0.52	0.81
30	0.12	0.40	0.40	0.70
35	0.08	0.15		0.59
40	0.04	-0.08		0.49
45		-0.28		

TABLE 6 (Cont'd)

(t) NGC 3623; Minor Axis

D 50"x4"

y	F2	F3	y	F2	F3
-95	-0.02	0.05	5	2.09	2.41
-90	0.09	0.15	10	1.97	2.32
-85	0.21	0.30	15	1.83	2.13
-80	0.33	0.46	20	1.71	1.85
-75	0.41	0.55	25		
-70	0.50	0.64	30		
-65	0.59	0.74	35	1.23	1.50
-60	0.72	0.84	40	1.23	1.54
-55	0.81	0.95	45	1.24	1.41
-50	0.92	1.18	50	1.06	1.25
-45	1.04		55	0.87	1.14
-40		1.62	60	0.77	1.03
-35	1.36	1.75	65	0.67	0.90
-30	1.48	1.82	70	0.59	0.74
-25	1.63	1.94	75	0.45	0.57
-20	1.76	2.09	80	0.35	0.49
-15	1.89	2.24	85	0.28	0.45
-10	2.01	2.36	90	0.19	0.41
- 5	2.11	2.49	95		0.35
0	2.20	2.61	100		0.21

(u) NGC 3623; Major Axis

D 12"x4"

x	F2	F3	x	F2	F3
-260	-0.12	-0.15	10	1.60	1.94
-250	0.00	-0.04	20	1.36	1.70
-240	0.20	0.07	30	1.14	1.53
-230	0.28	0.19	40	0.93	1.39
-220	0.28	0.29	50	0.84	1.27
-210	0.30	0.39	60	0.80	1.21
-200	0.35	0.49	70	0.79	1.17
-190	0.46	0.61	80	0.80	1.16
-180	0.72	0.75	90	0.86	1.15
-170	0.72	0.84	100	0.88	1.14
-160	0.69	0.86	110	0.74	1.09
-150	0.65	0.88	120	0.60	1.01
-140	0.64	0.90	130	0.50	0.93
-130	0.75	1.00	140	0.47	0.89
-120	0.91	1.12	150	0.52	0.92
-110	0.97	1.14	160	0.64	0.94
-100	0.91	1.12	170	0.64	0.92
- 90	0.85	1.12	180	0.54	0.85
- 80	0.83	1.14	190	0.44	0.77
- 70	0.85	1.16	200	0.33	0.69
- 60	0.92	1.22	210	0.23	0.61
- 50	1.00	1.30	220	0.13	0.53
- 40	1.10	1.42	230	-0.01	0.45
- 30	1.24	1.56	240	-0.18	0.37
- 20	1.37	1.72	250	-0.32	0.25
- 10	1.53	1.94	260	-0.43	0.08
0	1.92	2.51	270		-0.11

(v) NGC 3623; Major Axis

D 4"

x	F2	F3	x	F2	F3
-32	1.36		2	2.10	2.48
-30	1.40		4	2.02	2.41
-28	1.43	1.72	6	1.92	2.29
-26	1.46	1.74	8	1.84	2.20
-24	1.50	1.77	10	1.76	2.10
-22	1.53	1.80	12	1.71	2.04
-20	1.56	1.84	14	1.66	1.96
-18	1.58	1.89	16	1.61	1.93
-16	1.62	1.93	18	1.56	1.88
-14	1.67	1.97	20	1.52	1.84
-12	1.71	2.02	22	1.48	1.80
-10	1.77	2.06	24	1.43	1.75
- 8	1.87	2.17	26	1.40	1.71
- 6	1.95	2.29	28	1.37	1.67
- 4	2.07	2.40	30	1.34	1.65
- 2	2.12	2.46	32	1.31	1.64
0	2.13	2.50	34	1.29	

(w) NGC 4526; Minor Axis

D 12"x1"

y	F2	F3	y	F2	F3
- 36	-0.13		- 4	1.42	1.84
- 34	-0.06		- 2	1.62	2.00
- 32	0.01		0	1.74	2.14
- 30	0.08		2	1.40	1.88
- 28	0.15		4	1.28	1.69
- 26	0.21	0.59	5	1.28	1.67
- 24	0.29	0.64	6	1.27	1.63
- 22	0.39	0.72	8	1.17	1.51
- 20	0.47	0.81	10	1.04	1.38
- 18	0.59	0.93	12	0.91	1.29
- 16	0.69	1.02	14	0.81	1.20
- 14	0.80	1.12	16	0.72	1.11
- 12	0.89	1.23	18	0.66	1.00
- 10	0.99	1.37	20	0.60	0.91
- 8	1.12	1.47	22	0.53	0.81
- 6	1.24	1.61	24	0.46	0.70

TABLE 6 (Cont'd)

(w) NGC 4526; Minor Axis					
D 25"x4"					
y	F2	F3	y	F2	F3
-80		0.09	- 5	1.97	2.35
-75		0.18	0	2.29	2.66
-70		0.26	5	1.98	2.35
-65	-0.07	0.34	10	1.70	2.11
-60	-0.02	0.44	15	1.47	2.00
-55	0.04	0.53	20	1.28	1.78
-50	0.11	0.64	25	1.04	1.53
-45	0.23	0.78	30	0.85	1.39
-40	0.46	0.79	35	0.64	1.18
-35	0.71	0.99	40	0.45	0.96
-30	0.90	1.18	45	0.14	0.77
-25	1.10	1.37	50	-0.09	0.66
-20	1.37	1.62	55	-0.29	0.56
-15	1.59	1.82	60	-0.50	0.44
-10	1.88	2.02	65		0.36

(x) NGC 4526; Tracings Across Shadow Band					
D 12"x1"					
y	F2	F3	y	F2	F3
-1	1.65		- 6	1.32	1.64
-1.5	1.57		- 6.5	1.28	1.60
-2	1.50	1.86	- 7	1.26	1.58
-2.5	1.42	1.76	- 7.5	1.22	1.54
-3	1.39	1.67	- 8	1.19	1.51
-3.5	1.33	1.64	- 8.5	1.16	1.48
-4	1.31	1.65	- 9	1.14	1.45
-4.5	1.33	1.67	- 9.5	1.10	1.42
-5	1.34	1.68	-10	1.07	1.40
-5.5	1.33	1.68	-10.5		1.37

(y) NGC 4526; Major Axis					
D 6"x4"					
x	F2	F3	x	F2	F3
-115	-0.13		-10	1.27	1.71
-110	-0.08		- 5	1.67	1.97
-105	-0.03	0.43	0	1.93	2.21
-100	0.01	0.44	5	1.71	1.92
- 95	0.08	0.46	10	1.38	1.69
- 90	0.13	0.49	15	1.22	1.61
- 85	0.18	0.54	20	1.24	1.47
- 80	0.23	0.59	25	0.99	1.29
- 75	0.27	0.62	30	0.80	1.15
- 70	0.30	0.66	35	0.70	1.07
- 65	0.36	0.71	40	0.64	1.00
- 60	0.41	0.76	45	0.59	0.95
- 55	0.46	0.82	50	0.54	0.91
- 50	0.50	0.86	55	0.50	0.87
- 45	0.56	0.94	60	0.45	0.83
- 40	0.62	1.00	65		0.80
- 35	0.71	1.08	70		0.76
- 30	0.78	1.14	75		0.72
- 25	0.90	1.22	80		0.70
- 20	1.04	1.37	85		0.67
- 15	1.16	1.55			

paper and reading from this line the intensities at given points. It must be kept in mind that small irregularities are smoothed out in this way, even when they are real. The letters *a*, *b*, etc., in Table 6 serve as references to Figures 1–5, which are marked with the same letters.

For some nebulae, color measures were also made with a fixed diaphragm at various points of the nebula. As a rule, these measures yielded poor results because the telescope could not be guided during the measures. It is reasonable to suppose that the tracings were also influenced by the lack of guiding. To minimize this effect as much as possible, very long diaphragms were used for the tracings of some large nebulae; in this way the nucleus was always caught, even if not in the center of the diaphragm. When the size of the nebula was too small, this could not be done, and in these cases the nucleus was sometimes missed. These tracings were omitted from the discussion.

When the central intensities of the nebular tracings are compared with intensity measures of the nucleus made with fixed diaphragm in the same night, it appears that the latter values are always smaller than the former. This may have been caused by irregular guiding. Another explanation may be found in a too large scanning speed near the nucleus, where the intensity gradient is often very great. The differences between the nuclear values with fixed and with moving diaphragms vary between 0.04 and 0.20 mag. and are generally larger for F2 than for F3. It seems difficult to explain this latter difference.

The general conclusion of this paper is that the attempt to measure the intensity distribution of the nebulae photoelectrically has succeeded, although for a variety of reasons the accuracy of the measures is less than that anticipated from photoelectric observations. The authors regret that, because of unforeseen circumstances, publication was delayed until now.

In a forthcoming publication a discussion of these measures will be given, in combination with intensity distributions derived photographically.

REFERENCES

Evans, David S. 1951, *M.N.*, **111**, 526–536.
———. 1952, *ibid.*, **112**, 606–613.
Hubble, Edwin. 1930, *Ap. J.*, **71**, 231–276.
Redman, R. O., and Shirley, E. G. 1938, *M.N.*, **98**, 613–623.
Shapley, Harlow, and Ames, Adelaide. 1932, *Harvard Ann.*, **88**, No. 2, 41–75.
Vaucouleurs, Gérard de. 1948, *Ann. d'ap.*, **11**, 247–287.